



Since January 2020 Elsevier has created a COVID-19 resource centre with free information in English and Mandarin on the novel coronavirus COVID-19. The COVID-19 resource centre is hosted on Elsevier Connect, the company's public news and information website.

Elsevier hereby grants permission to make all its COVID-19-related research that is available on the COVID-19 resource centre - including this research content - immediately available in PubMed Central and other publicly funded repositories, such as the WHO COVID database with rights for unrestricted research re-use and analyses in any form or by any means with acknowledgement of the original source. These permissions are granted for free by Elsevier for as long as the COVID-19 resource centre remains active.



An alternative $-1/+2$ open reading frame exists within viral N^{pro}(1–19) region of bovine viral diarrhea virus SD-1

Zhen-Chuan Fan*, R. Curtis Bird

Department of Pathobiology, College of Veterinary Medicine, Auburn University, Auburn, AL 36849-5519, United States

ARTICLE INFO

Article history:

Received 7 July 2011

Received in revised form 22 October 2011

Accepted 27 October 2011

Available online 4 November 2011

Keywords:

Flavivirus

Pestivirus

BVDV

N^{pro}

Frameshift ORF

ABSTRACT

We previously reported the engineering of an N^{pro}-disrupted bovine viral diarrhea virus (BVDV), BSD1-N^{pro}/eGFP2A (Fan and Bird, 2008a). Here, we report that BSD1-N^{pro}/eGFP2A survives a single nucleotide missing in its C-terminal eGFP region. By using our established reverse genetics system for BVDV, we confirm that the viral mutant is rescued through a $-1/+2$ ORF initiated in the N^{pro}(1–19)/eGFP region of the mutant viral genome. We furthermore uncover that this event occurs in the N^{pro}(1–19) region of BVDV strain SD-1. The rescued viral mutant showed dramatic reductions in levels of both viral RNA and viral protein in host cells. Although the mutant is similar to the native strain in viral kinetics, the peak yield of the mutant is decreased dramatically. These findings reveal the existence of an alternative $-1/+2$ ORF in the N^{pro}(1–19) region during the replication of BVDV and open a new avenue to understand the life cycle and pathogenesis of pestiviruses.

© 2011 Elsevier B.V. All rights reserved.

1. Introduction

The *Flaviviridae* family includes three genera: flavivirus, hepatitis virus and pestivirus (Lindenbach and Rice, 2003). Bovine viral diarrhea virus (BVDV) is one of the major pathogens causing significant economic loss of cattle production and reproduction the world wide. As the prototype virus of the pestivirus genus, BVDV has a genome consisting of a single-stranded, positive-oriented RNA molecule of approximately 12.3 kb. BVDV, like other members in the *flaviviridae* family, contains a single open reading frame (ORF) that is flanked with a 5'-nontranslated region (5'-NTR) and a 3'-untranslated region (3'-NTR) and encodes a single polyprotein. The viral polyprotein is initiated cap-independently from an internal ribosome entry site (IRES) located in the 5'-NTR and proteolytically cleaved to yield the viral proteins, specifically for BVDV, four structural proteins (core, E¹^{ns}, E1 and E2) and at least seven non-structural proteins (N^{pro}, P7, NS2/3, NS4A, NS4B, NS5A, and NS5B) (Lindenbach and Rice, 2003).

Unlike other species in *flaviviridae* family, pestiviruses share a unique proximal N-terminal leader autoprotease, N^{pro}. N^{pro} is a cysteine proteinase which cleaves at its own C-terminal cysteine and serine dipeptide site to release the N-terminus of viral capsid (C) protein (Rumenapf et al., 1998; Stark et al., 1993). Other

than this, N^{pro} has not been found to be essential for viral replication (Fan and Bird, 2008a; Tratschin et al., 1998). Currently, whether or not this viral protein participates in viral pathogenesis remains unknown. However, recent evidence from both *in vivo* and *in vitro* studies indicates that pestivirus N^{pro} is a pivotal factor in inhibiting the host innate immune system (Bauhofer et al., 2007; Chen et al., 2007; Gil et al., 2006; Hilton et al., 2006; Horscroft et al., 2005; La Rocca et al., 2005; Ruggli et al., 2005; Seago et al., 2007) and might be a critical determinant for the establishment of persistent fetal infection of BVDV (Meyers et al., 2007).

BVDV share the molecular and virological similarities with hepatitis C virus (HCV), the sole member of hepatitis virus genus and has been adopted a model virus for investigating viral replication mechanism and virulent determinants of HCV (Baginski et al., 2000) until 2005 when a recombinant HCV can be completely propagated in cell culture (Lindenbach et al., 2005). Interestingly, numerous studies had showed that an additional HCV protein of approximately 16 kDa is biosynthesized from the initiator codon of the viral polyprotein sequence followed by a $+1/-2$ translational ribosomal frameshift operating in the region of core protein codons (Baril and Brakier-Gingras, 2005; Boulant et al., 2003; Choi et al., 2003; Cristina et al., 2005; McMullan et al., 2007; Rijnbrand et al., 2001; Varaklioti et al., 2002; Vassilaki and Mavromara, 2003; Walewski et al., 2001; Xu et al., 2001). Over the past few years, translational ribosome frameshift was also detected to exist in the replication of many members of flavivirus genus such as Dengue virus (Firth and Atkins, 2009; Firth et al., 2010), Japanese Encephalitis Virus (Melian et al., 2010), West Nile virus (Youn et al., 2010). However,

* Corresponding author at: Obesita & Algaegen Inc., 3631 Vienna Dr., College Station, TX 77845, United States. Tel.: +1 334 497 1780; fax: +1 979 446 0687.

E-mail addresses: fanzhen@obesita-algaegen.com, fanzc1974@hotmail.com (Z.-C. Fan).

to the best of our knowledge, there is no evidence so far to show that overlapping ORF exists in the life cycle of pestiviruses.

In this study, we initially find that a mutant reporter BVDV survives a frameshift mutation at its 3'-end of the eGFP coding region, suggesting the possible existence of an alternative ORF during viral replication. We further show evidence that a -1/+2 ORF exists in BVDV genome and initiates in viral N^{pro}(1–19) coding region, thus reporting for the first time that overlapping ORF also exists in the life cycle of pestiviruses.

2. Materials and methods

2.1. Cell and viruses

Madin–Darby bovine kidney (MDBK) cells were cultured in Dulbecco's modified Eagles medium (DMEM) supplemented with 10% heat-inactivated equine serum, 2 μ M of L-glutamine, 200 U/ml of penicillin, and 0.2 mg/ml of streptomycin. Cells were maintained at 37 °C and 5% CO₂. Native BVDV SD-1, recombinant BVDV BSD1 and BVDV mutant BSD1-N^{pro}/eGFP2A have been described previously (Deng and Brock, 1992; Fan et al., 2008). BSD1-N^{pro}/eGFP2A-c1044 Δ and BSD1-g442 Δ were generated as described below.

2.2. Plasmid constructs

Standard procedures for cloning were performed as described previously (Sambrook and Russell, 2001). The sequence of the plasmids was confirmed by direct nucleotide sequencing. Numbering of nucleotides and amino acids herein refers to the genome sequence of BVDV mutant BSD1-N^{pro}/eGFP2A (Fan et al., 2008). Plasmids pACSD1, pACXF, pFAN16, pBADFP, pBSD1 pBSD1-N^{pro}/eGFP2A were described previously (Fan and Bird, 2008a,b; Fan et al., 2008). For construction of pBSD1-N^{pro}/eGFP2A-1 and pBSD1-N^{pro}/eGFP2A-2, the mutation was introduced into pFAN16 by site-directed mutagenesis (Stratagene), resulting in pFAN20 and pFAN21, respectively. The 4.5 kb XbaI-FseI fragment derived from pFAN20 or pFAN21 and a 8.1 kb fragment of pBADFP were then cloned into the XbaI-PacI sites of pBSD1 resulting in pBSD1-N^{pro}/eGFP2A-1 and pBSD1-N^{pro}/eGFP2A-2, respectively. pBSD1-g442 Δ was created by similar method except that the mutation was instead introduced into pACXF by site-directed mutagenesis. Detailed information about primers and cloning procedure are available upon request.

2.3. Rescue and titration of recombinant viruses

As described previously (Fan and Bird, 2008b), *in vitro* transcription and transfection of MDBK cells were performed with a T7-MEGAscript kit (Ambion, Austin, TX) and Gene Pulser apparatus (Bio-Rad, Hercules, CA), respectively. Rescued viruses were passaged 10 times, titrated, and stocked as working viruses. Virus titer was determined by focus forming assay as detailed previously (Fan and Bird, 2008b). Infection of MDBK cells was performed at a multiplicity of infection (MOI) of 1 focus forming unit (FFU)/cell unless otherwise specified.

2.4. Viral RNA extraction and standard RT-PCR

Viral RNA extraction and two-step RT-PCR were performed as described previously (Fan et al., 2008). Anti-sense primer BVD1172 (5'-CTACGGCCAATATTGCC-3') was used for first strand synthesis in RT step and primer pair BVD424P (5'-CAAACAAAACCGTCGG-3') and BVD1172 was used for PCR amplification with following parameters: 95 °C for 2 min followed by 45 cycles of 95 °C for 1 min,

57 °C for 45 s, and 72 °C for 90 s. RT-PCR products were verified by both agarose gel electrophoresis and nucleotide sequencing.

2.5. Determination of virus growth kinetics

Viral growth kinetics was determined as described previously (Fan et al., 2008). In detail, monolayer of MDBK Cells (~60% confluent) was infected with viruses at both a high MOI of 1 FFU/cell and a low MOI of 0.1 FFU/cell in each well of a 24-well plate. After 1-h absorption, the cells were washed twice with PBS and incubated at 37 °C in fresh complete medium. At various time points p.i., progeny virions were collected by three freeze-thaw cycles and titered by focus forming assay.

2.6. Quantitation of viral RNA genome

Quantification of viral RNA genome was performed in a time-course style by qRT-PCR performed on a LightCycler instrument (Roche, Mannheim, Germany) with a QuantiTect™ SYBR® green RT-PCR kit (Qiagen) as described previously (Fan et al., 2008). The RT step was performed in a 50 μ l system harboring either sense primer of BVD424 at 42 °C for 1 h followed by 95 °C for 10 min to heat-inactivate reverse transcriptase and to activate the HotStarTag DNA polymerase. The assay contains 2.5 μ g of extracted RNA, 1 μ M of primer, and RT-PCR mix (Qiagen). After that, complementary primer BVD764N (5'-TGCCGTCAGTCCAGTTA-3') was added to the reactions and PCR amplifications were performed for 40 cycles (95 °C for 30 s, 57 °C for 45 s, and 72 °C for 1 min).

2.7. Quantitation of viral E2 protein

To quantify the expression of viral E2 protein, virus- and mock-infected MDBK cells (1×10^5) were collected at 60 h p.i. by centrifugation at 1200 rpm for 2 min and washed twice with PBS. Cells were labeled with primary anti-E2 Mabs D89 (1:300 dilution, VMRD, Pullman, WA) and secondary Alexa Fluor® 680-conjugated rabbit anti-mouse IgG (H+L) (1:500 dilution, Molecular Probes, Eugene, OR) as described previously (Fan et al., 2008). Fixed cells were resuspended in 0.5 ml PBS and analyzed by flow cytometry with a MoFlo 8-color flow cytometer & high-performance sorter (Dakocytometry).

2.8. Quantitation of green fluorescence protein signal

MDBK cells (1×10^6) were infected with BVDV mutants as well as wt SD-1-infected MDBK cells and mock-MDBK cells as negative controls. At 12, 36 and 60 h p.i., respectively, cells were analyzed by FACS using a MoFlo 8-color flow cytometer & high-performance sorter (Dakocytometry) with an excitation spectrum of 488 nm as described previously (Fan et al., 2008). Accumulation of GFP protein was reflected by MFI of the fluorescence-positive MDBK cells.

2.9. Fluorescence microscopy and visualization of the cells

The detail about the cell seeding, virus infection, cell incubation, and slide preparation has been described previously (Fan et al., 2008). At the desired time points, cells were washed with PBS. The slides were then mounted and viewed with an epi-fluorescence-equipped Nikon Eclipse E600W microscope. Photos were captured using an RT-Slide Spot digital camera (Diagnostic Instruments, Sterling Heights, MI) at 200 \times amplification with an exposure time of 45 s.

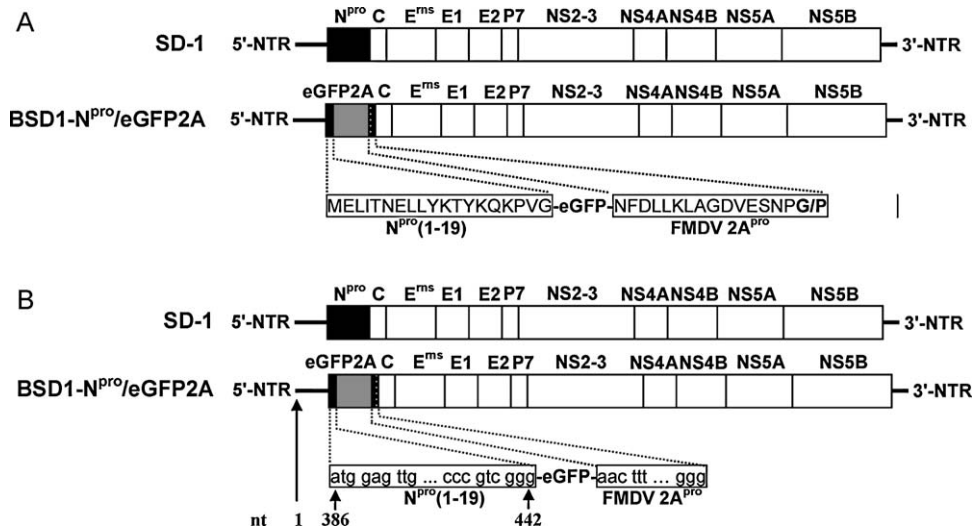


Fig. 1. Schematic representative of the constructs used for *in vitro* transcription. (A) Schematic representative of part of the amino acid of parental BVDV SD-1 and pBSD1-N^{pro}/eGFP2A. The amino acids of N^{pro}, N^{pro}-2A, eGFP2A and C are marked with boxes. The first 19 amino acid residues of N^{pro} protein are marked with bond. The 17 amino acid peptide of FMDV 2A^{pro} is marked with underline. The lactic amino acid represents that substitution of V to P in pBSD1-N^{pro}/eGFP2A. (B) Schematic representative of part of the nucleotide sequence of parental BVDV SD-1 and pBSD1-N^{pro}/eGFP2A. The nucleotide sequences of N^{pro}-2A, N^{pro}, eGFP2A and C are marked with boxes. Both underline and bond represent the N^{pro}/2A, 2A/eGFP, eGFP/2A, and 2A/C junctions.

2.10. SDS-PAGE and western blotting

Cell seeding, virus infection, cell incubation and collection have been described previously (Fan et al., 2008). 40 µg of cell lysates were separated on an 8–16% SDS-PAGE gel (Precise protein gel, Pierce) and transferred to a PVDF membrane (Sigma–Aldrich, South San Francisco, CA). The membrane was blocked for 1 h, incubated with mouse anti-GFP Mab JL-8 (1:1000 dilution, Clontech, Palo Alto, CA) for 2 h, washed with PBS followed incubation with alkaline phosphatase-conjugated, affinity purified goat anti mouse immunoglobulins (IgG, IgA, IgM) (1:1000 dilution, MP Biomedicals, Aurora, OH) for 1 h. After washing with PBS, green fluorescent protein was detected with an alkaline phosphatase substrate (Bio-Rad) for 10 min and recorded with a Canon Powershot A80 digital camera (Canon USA Inc., Lake Success, NY).

3. Results

3.1. Rescue of an infectious reporter BVDV lacking a single nucleotide in its genome

As reported previously (Fan and Bird, 2008a), BSD1-N^{pro}/eGFP2A is an engineered N^{pro}-disrupted reporter BVDV derived from an infectious BAC cDNA clone, pBSD1-N^{pro}/eGFP2A, with a NCP BVDV SD-1 background (Deng and Brock, 1992). BSD1-N^{pro}/eGFP2A was designed to express a chimeric eGFP2A protein that was introduced into viral polyprotein by replacing the whole N^{pro} protein except its first 19 amino acids. The eGFP2A was created with a foot-and-mouth disease virus 2A protease (FMDV 2A^{pro}) attached to C-terminus of an enhanced green fluorescent protein (eGFP) (Fig. 1A and B). This design assures the successful release of eGFP2A chimera from viral nascent polyprotein precursor by taking advantage of FMDV 2A^{pro} protease activity (Fan and Bird, 2008a; Fan et al., 2008; Ryan and Drew, 1994; Ryan et al., 1991). During one of our attempts to optimize the assay, infectious viruses were rescued after MDBK cells were transfected with the run-off RNAs *in vitro* transcribed from pBSD1-N^{pro}/eGFP2A (data not shown). RT-PCR of viral RNA using primer pair BVD424 and BVD1172 that target the viral N^{pro}(1–19)/eGFP2A/C coding

region (nt 390–1172, by reference to the nucleotides of BSD1-N^{pro}/eGFP2A) identified a unique cDNA band of approximately 1.1 kb (Fig. 2A). Direct nucleotide sequencing of the cDNA products found a single cytosine nucleotide missing at nt 1044 (c1044Δ) (Fig. 2B). Nucleotide sequencing did not find any other mutation(s) in viral genome of the rescued virus (Data not shown). These results reveal that a mutant viral genome is the solely infectious RNA molecule present in the infected MDBK cells. The acquired mutation of the mutant virus is located in the 3'-end of the viral eGFP region. Here, we name the rescued mutant virus as BSD1-N^{pro}/eGFP2A-c1044Δ.

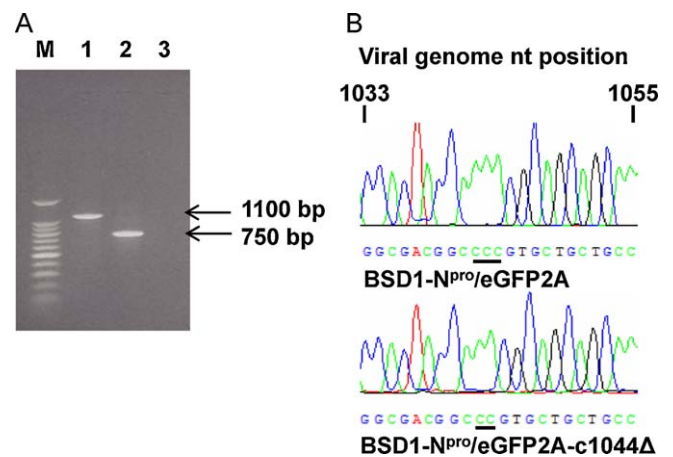


Fig. 2. BSD1-N^{pro}/eGFP2A-c1044Δ genome lacks a cytosine nucleotide at nt 1044. (A) Complementary DNA fragments amplified from viral RNA of BSD1-N^{pro}/eGFP2A-c1044Δ and BSD1 by RT-PCR. Primer pair used for RT-PCR was BVD424P and BVD1172. M: 1 kb DNA ladder; Lane 1: cDNA fragment amplified from viral RNA of BSD1-N^{pro}/eGFP2A-c1044Δ with an expected size of 1100 bp. Lane 2: cDNA fragment amplified from viral RNA of BSD1 with an expected size of 750 bp; and Lane 3: blank reaction (no templates) as negative control. (B) Lack of a cytosine nucleotide at nt 1044 was detected at the 3'-end of eGFP2A coding region of BSD1-N^{pro}/eGFP2A-c1044Δ (shown as underlined letters on the bottom of each panel). The shown nucleotide sequences of partial viral genomes were amplified from viral RNAs of BSD1-N^{pro}/eGFP2A-c1044Δ and BSD1-N^{pro}/eGFP2A. The numbers show the nucleotide positions referring to the genomic sequence of BSD1-N^{pro}/eGFP2A.

3.2. Existence of an additional $-1/+2$ ORF in the infectious reporter BVDV

Nucleotide sequence analysis shows that mutation c1044 Δ causes a frameshift with the formation of a premature stop codon (TGA at nt 1069–1071) in eGFP coding region, 54 nucleotides before the FMDV 2A^{Pro} sequence (Fig. 3). The appearance of this stop codon in the original viral 0/0 ORF of BSD1-N^{Pro}/eGFP2A-c1044 Δ is supposed to direct the generation of an unstable, fluorescence-deficient variant of eGFP protein that is C-terminal 18-AA truncated (Dopf and Horiagon, 1996) and no viable viruses should be generated (Fig. 3). Based on this observation, we postulated that BSD1-N^{Pro}/eGFP2A-c1044 Δ can be rescued only through a $-1/+2$ ORF that must exist and initiate in the coding region of either N^{Pro}(1–19) or eGFP. Furthermore, it is obvious that, no matter which coding region this event falls in, a functional eGFP protein is not supposed to be produced. As expected, different from BSD1-N^{Pro}/eGFP2A-infected MDBK cells that showed a time-dependent, rapid elevation of green fluorescent protein as measured by a combination of fluorescence microscopy (FM), FACS and western blotting at 12, 36, and 60 h post infection (p.i.) (Fig. 4A–C) (Fan et al., 2008), MDBK cells infected with BSD1-N^{Pro}/eGFP2A-c1044 Δ did not show any fluorescence signal as determined by both IFM and FACS as checked at all three time points (Fig. 4A and B). In addition, green fluorescent protein was not detectable in the mutant virus-infected cells as checked in a time-course western blotting assay (Fig. 4C). Taken together, these data conclusively reveals the existence of an additional ORF in viral N^{Pro}(1–19)/eGFP region.

3.3. Confirmation of a $-1/+2$ ORF within the N^{Pro}(1–19)/eGFP coding region

To further verify the above observation and hypothesis, two cDNA clones containing a single cytosine nucleotide deletion at nt 1044 (pBSD1-N^{Pro}/eGFP2A-1) or double cytosine nucleotide deletions at nt 1043 and 1044 (BSD1-N^{Pro}/eGFP2A-2) were created on the base of pBSD1-N^{Pro}/eGFP2A. Together with pBSD1-N^{Pro}/eGFP2A (Fan and Bird, 2008a), three constructs represent 0/0, $-1/+2$, and $+1/-2$ frames, respectively (Fig. 5A). As shown in Fig. 5B, focus forming assay indicated that infectious viruses (passage 0) were successfully rescued from the transcripts derived from pBSD1-N^{Pro}/eGFP2A and pBSD1-N^{Pro}/eGFP2A-1 but not from pBSD1-N^{Pro}/eGFP2A-2. After five additional blind passages in MDBK cells with the culture supernatant, the rescued mutant virus was confirmed to be deficient in GFP generation as assayed with a western blotting assay (Fig. 5C). The N^{Pro}(1–19)/eGFP2A/C coding sequence was stably retained in viral genomes as analyzed with RT-PCR of viral RNA extracted from the viruses both at passage 5 (Fig. 5D). Nucleotide sequencing of the RT-PCR products demonstrated that the rescued viruses retain the original nucleotide sequence of the N^{Pro}(1–19)/eGFP2A/C region as engineered (Fig. 5E). These results confirmed our observation that an additional ORF exists in the viral N^{Pro}(1–19)/eGFP region. Furthermore, these data indicates that it is a $-1/+2$ ORF but not a $+1/-2$ ORF that exists during viral replication, initiates in viral N^{Pro}(1–19)/eGFP coding region, and alternatively directed the rescue of BVDV mutant BSD1-N^{Pro}/eGFP2A-c1044 Δ .

3.4. Analysis of the mutation impact on replication of the viable recombinant virus

BSD1-N^{Pro}/eGFP2A, similar to native SD-1 strain, can reach a peak titer of approximately 4.1×10^6 FFU/ml only after five passages (Fan and Bird, 2008a). BSD1-N^{Pro}/eGFP2A-c1044 Δ approached a maximum virus titer after five passages in MDBK cells but the virus titer number was only 6.3×10^3 FFU/ml (Fig. 6A).

Viral growth kinetics showed that two viruses all reached a peak virus yield at 60 h p.i. However, BSD1-N^{Pro}/eGFP2A-c1044 Δ was up to 3.3 log₁₀ lower than BSD1-N^{Pro}/eGFP2A in maximum titer achievement (Fig. 6B). To elucidate the underlying mechanism of these observations, we measured the accumulation of viral RNA genome and viral E2 protein. Quantitative real-time RT-PCR assay indicated that BSD1-N^{Pro}/eGFP2A-c1044 Δ had plus-strand viral RNA accumulation at a much lower level than BSD1-N^{Pro}/eGFP2A as measured at 12, 36, and 60 h p.i., respectively (Fig. 6C). FACS assay indicated that the viral E2 level of BSD1-N^{Pro}/eGFP2A-c1044 Δ was only approximately 62% of that of BSD1-N^{Pro}/eGFP2A as checked at 60 h p.i. (Fig. 6D). These results suggest that either viral genome replication, viral protein translation efficacy, or both represented by the $-1/+2$ ORF of BSD1-N^{Pro}/eGFP2A-c1044 Δ was much lower than that of the original 0/0 ORF represented by BSD1-N^{Pro}/eGFP2A. These findings explained why BSD1-N^{Pro}/eGFP2A-c1044 Δ has a lower virus titer than BSD1-N^{Pro}/eGFP2A because its assembly was impaired by the reduced viral RNA and protein products in infected MDBK cells.

3.5. The $-1/+2$ ORF initiates in N^{Pro}(1–19) region of the native virus SD-1

To determine if the $-1/+2$ ORF initiates in the N^{Pro}(1–19) coding region of the native SD-1 strain, a cDNA clone pBSD1-c442 Δ containing a single guanine-nucleotide deletion at nt 442 was created based on pBSD1 (Fan and Wang, 2009) to represent a $-1/+2$ ORF (Fig. 7A). Together with pBSD1 representing the original viral 0/0 ORF, the *in vitro* transcripts synthesized from these two constructs were electroporated into MDBK cells and infectious viruses (defined as passage 0) were successfully obtained. After five additional blind passages in MDBK cells with the culture supernatant, the rescued viruses were verified to be infectious as assayed with IFA (Fig. 7B). BSD1-g442 Δ approached a maximum virus titer after five passages in MDBK cells but the virus titer number was only 2.1×10^3 FFU/ml (Fig. 7C). Analysis of viral growth kinetics indicated that the viral growth pattern was comparable between BSD1-g442 Δ and BSD1 and both viruses reached a peak virus yield at 60 h p.i. However, BSD1-g442 Δ was up to 4.3 log₁₀ lower than BSD1 in maximum titer achievement (Fig. 7D). Quantitative real-time RT-PCR assay indicated that BSD1-g442 Δ had a much lower plus-strand viral RNA accumulation than BSD1 as measured at 12, 36, and 60 h p.i., respectively (Fig. 7E). Event at 60 h p.i., BSD1-g442 Δ only has a viral RNA genome level approximately 45% of that of BSD1. FACS assay indicated that the level of viral E2 protein of BSD1-g442 Δ was much lower than that of BSD1 at all three checked time points. This viral mutant shows a viral E2 protein level approximately 59% of that of BSD1 as measured at 60 h p.i. (Fig. 7F). These results reveal that an additional $-1/+2$ ORF initiates in viral N^{Pro}(1–19) region of the native BVDV SD-1 and directs the rescue of an infectious BVDV mutant, BSD1-g442 Δ . However, the efficacy for viral RNA and protein production of this frame is much lower than the original 0/0 frame of BVDV SD-1.

4. Discussion

In this study, we identified an additional $-1/+2$ ORF existing during the replication of a recombinant reporter BVDV, BSD1-N^{Pro}/eGFP2A (Fan and Bird, 2008a). BSD1-N^{Pro}/eGFP2A is characteristic of a disrupted N^{Pro} protein (N^{Pro}1–19) with its most C-terminal amino acids replaced with a reporter protein chimera, eGFP2A. The eGFP2A chimera was designed to consist of eGFP and FMDV 2A protease in such a way that eGFP2A can be cleaved from the viral precursor polyprotein of BSD1-N^{Pro}/eGFP2A and can be maintained stably in infected-MDBK cells (Fan and Bird, 2008a;

```

406 ATGGAGTTGATTACAAATGAACTTTTATACAAAACATACAAAACAAAACCCGTGGGGCCC BSD1-NP19/eGFP2A (0/0)
1 M E L I T N E L L Y K T Y K Q K P V G P
406 ATGGAGTTGATTACAAATGAACTTTTATACAAAACATACAAAACAAAACCCGTGGGGCCC BSD1-NP19/eGFP2A-c1044Δ (-1/+2)
1 M E L I T N E L L Y K T Y K Q K P V G P

466 ATGGTGAGCAAGGGCGAGGAGCTGTTTACCGGGGTGGTGCCCATCTGGTTCGAGCTGGAC
21 M V S K G G E E L F T G V V P I L V E L D
466 ATGGTGAGCAAGGGCGAGGAGCTGTTTACCGGGGTGGTGCCCATCTGGTTCGAGCTGGAC
21 M V S K G E E L F T G V V P I L V E L D

526 GCGACGTAAACGGCCACAAGTTCAGCGTGTCCGGCGAGGGCGAGGGCGATGCCACCTAC
41 G D V N G H K F S V S G E G E G D A T Y
526 GCGACGTAAACGGCCACAAGTTCAGCGTGTCCGGCGAGGGCGAGGGCGATGCCACCTAC
41 G D V N G H K F S V S G E G E G D A T Y

586 GGCAAGCTGACCCTGAAGTTCATCTGCACCACCGGCAAGCTGCCCGTGCCTGGCCACC
61 G K L T L K F I C T T G K L P V P W P T
586 GGCAAGCTGACCCTGAAGTTCATCTGCACCACCGGCAAGCTGCCCGTGCCTGGCCACC
61 G K L T L K F I C T T G K L P V P W P T

646 CTCGTGACCACCCTGACCTACGGCGTGCAGTGCTTCAGCCGCTACCCGACCACATGAAG
81 L V T T L T Y G V Q C F S R Y P D H M K
646 CTCGTGACCACCCTGACCTACGGCGTGCAGTGCTTCAGCCGCTACCCGACCACATGAAG
81 L V T T L T Y G V Q C F S R Y P D H M K

706 CAGCAGCACTTCTTCAAGTCCGCCATGCCCGAAGGCTACGTCCAGGAGCGCACCATCTTC
101 Q H D F F K S A M P E G Y V Q E R T I F
706 CAGCAGCACTTCTTCAAGTCCGCCATGCCCGAAGGCTACGTCCAGGAGCGCACCATCTTC
101 Q H D F F K S A M P E G Y V Q E R T I F

766 TTCAAGGACGACGGCAACTACAAGACCCGCGCCGAGGTGAAGTTCGAGGGCGACACCCTG
121 F K D D G N Y K T R A E V K F E G D T L
766 TTCAAGGACGACGGCAACTACAAGACCCGCGCCGAGGTGAAGTTCGAGGGCGACACCCTG
121 F K D D G N Y K T R A E V K F E G D T L

826 GTGAACCGCATCGAGCTGAAGGGCATCGACTTCAAGGAGGACGGCAACATCTGGGGCAC
141 V N R I E L K G I D F K E D G N I L G H
826 GTGAACCGCATCGAGCTGAAGGGCATCGACTTCAAGGAGGACGGCAACATCTGGGGCAC
141 V N R I E L K G I D F K E D G N I L G H

886 AAGCTGGAGTACAACTACAACAGCCACAACGCTCTATATCATGGCCGACAAGCAGAAGAAC
161 K L E Y N Y N S H N V Y I M A D K Q K N
886 AAGCTGGAGTACAACTACAACAGCCACAACGCTCTATATCATGGCCGACAAGCAGAAGAAC
161 K L E Y N Y N S H N V Y I M A D K Q K N

946 GGCATCAAGGTGAACTTCAAGATCCGCCACAACATCGAGGACGGCAGCGTGCAGCTCGCC
181 G I K V N F K I R H N I E D G S V Q L A
946 GGCATCAAGGTGAACTTCAAGATCCGCCACAACATCGAGGACGGCAGCGTGCAGCTCGCC
181 G I K V N F K I R H N I E D G S V Q L A

1006 GACCACTACCAGCAGAACACCCCCATCGGGCGACGGCCCGGTGCTGCTGCCCGACAACCAC
201 D H Y Q Q N T P I G D G P V L L P D N H
1006 GACCACTACCAGCAGAACACCCCCATCGGGCGACGGCCCGGTGCTGCTGCCCGACAACCAC
201 D H Y Q Q N T P I G D G P C C C P T T T

1066 TACCTGAGCACCCTCGCCCTGAGCAAAGACCCCAACGAGAAGCGCGATCACATGGTCC
221 Y L S T Q S A L S K D P N E K R D H M V L
1066 ACCTGAGACCCAGTCCGCCCTGAGCAAAGACCCCAACGAGAAGCGCGATCACATGGTCC
221 T *

```

Fig. 3. Mutation c1044Δ leads to the formation of a premature stop codon in mutant viral genome. Comparison of nucleotide sequences and amino acids deduced from the N^{P19}(1–19)/eGFP sequence of BSD1-N^{P19}/eGFP2A and BSD1-N^{P19}/eGFP2A-c1044Δ. The numbers on the left show that position of nucleotides and amino acids. The underlined letters show where the single cytosine nucleotide missing is in the BSD1-N^{P19}/eGFP2A-c1044Δ genome. The boxed TGA represents the premature stop codon formed in the eGFP region due to a frameshift mutation in BSD1-N^{P19}/eGFP2A-c1044Δ genome.

Fan et al., 2008). Failure to obtain such a recombinant virus in one of our attempts showed us a very interesting phenomenon. Namely, infectious viruses were indeed obtained, however green fluorescent protein was not detectable. Direct nucleotide sequencing identified a cytosine nucleotide missing at nt 1044 (c1044Δ) of the genome of the rescued virus. Since the mutation causes a frameshift with formation of a premature stop codon (TGA at nt 1069–1071) in C-terminal eGFP about 18 AA before FMDV 2A^{P19} a C-terminal 18 amino acid-truncated eGFP protein are supposed to be translated from the original viral 0/0 ORF. This finding explained why functional GFP protein was not detectable in this case because C-terminal truncation of even 6 amino acids already results in a complete fluorescence loss of the mutant GFP protein (Dopf and

Horiagon, 1996). It is interesting to see that the mutant GFP protein was even not detected in the western blotting assay. This happened probably due to the fact that the antibody applied in the assay cannot recognize the C-terminal 18 AA truncated mutant GFP protein. We actually tested several other commercially available anti-GFP antibodies and they all failed to detect the mutant GFP protein.

Since mutation c1044Δ causes the formation of a premature stop codon in the C-terminal eGFP region the generation of infectious viruses is not expected from its original 0/0 ORF of viral genome. It was already known that ribosome skipping is actively promoted by FMDV 2A^{P19} sequence and insertion of this small sequence in viral genome leads to the efficient release of its downstream protein (Donnelly et al., 2001; Funston et al., 2008).

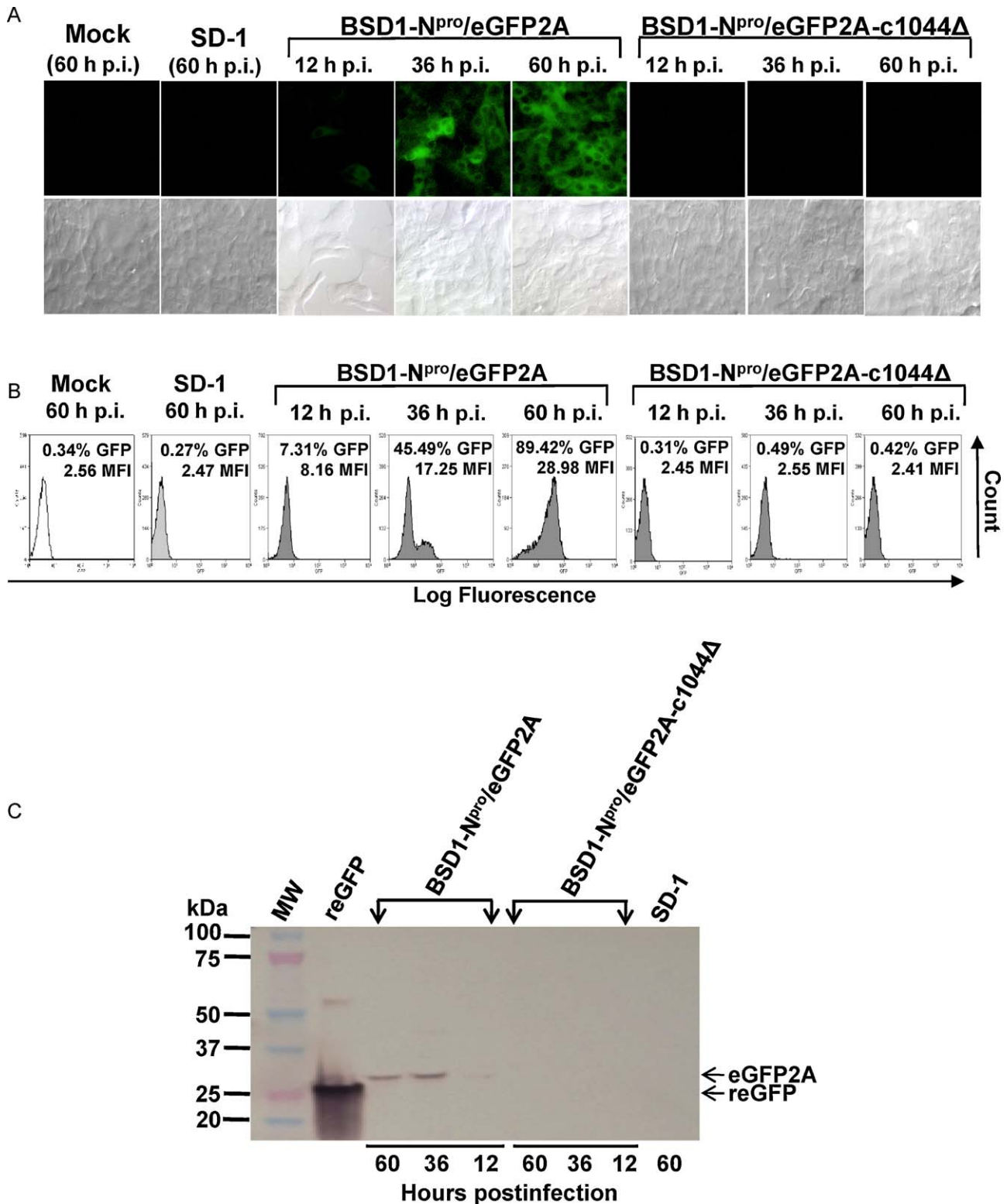


Fig. 4. Functional green fluorescent protein was not generated in mutant virus-infected MDBK cells. (A) MDBK cells were infected with BSD1-N^{pro}/eGFP2A or BSD1-N^{pro}/eGFP2A-c1044Δ. At 12, 36 and 60 h p.i., respectively, GFP fluorescence was detected by fluorescence microscopy (upper panel). Bottom pictures show the phase contrast images correspond to photos in the upper panel. Mock- and SD-1-infected MDBK cells collected at 60 h p.i. were used as negative controls. (B) Mock- and virus-infected MDBK cells were collected exactly the same as described above and GFP fluorescence of the cells was quantified by FACS assay. The percentage of the population and mean fluorescence intensity (MFI) of GFP fluorescence-positive cells are noted for each panel. (C) Virus-infected MDBK cells were collected exactly the same as described above. Here, lysates of SD-1-infected MDBK cells and recombinant GFP protein were used as negative and positive controls, respectively. Green fluorescent protein was detected by western blotting with a monoclonal anti-GFP antibody, JL-8. Lane 1: Molecular mass standard (MW) in kilodaltons (kDa, indicated on the left); Lane 2: recombinant eGFP protein control; Lane 3 to Lane 5: 40 μg of lysate of BSD1-N^{pro}/eGFP2A-infected MDBK cells collected at different time points p.i. (indicated on the bottom); Lane 6 and Lane 8: 40 μg of lysates of BSD1-N^{pro}/eGFP2A-c1044Δ-infected MDBK cells collected at different time points p.i. (indicated on the bottom); and Lane 9: 40 μg of lysates of SD-1-infected MDBK cells collected at 60 h p.i. as negative control.

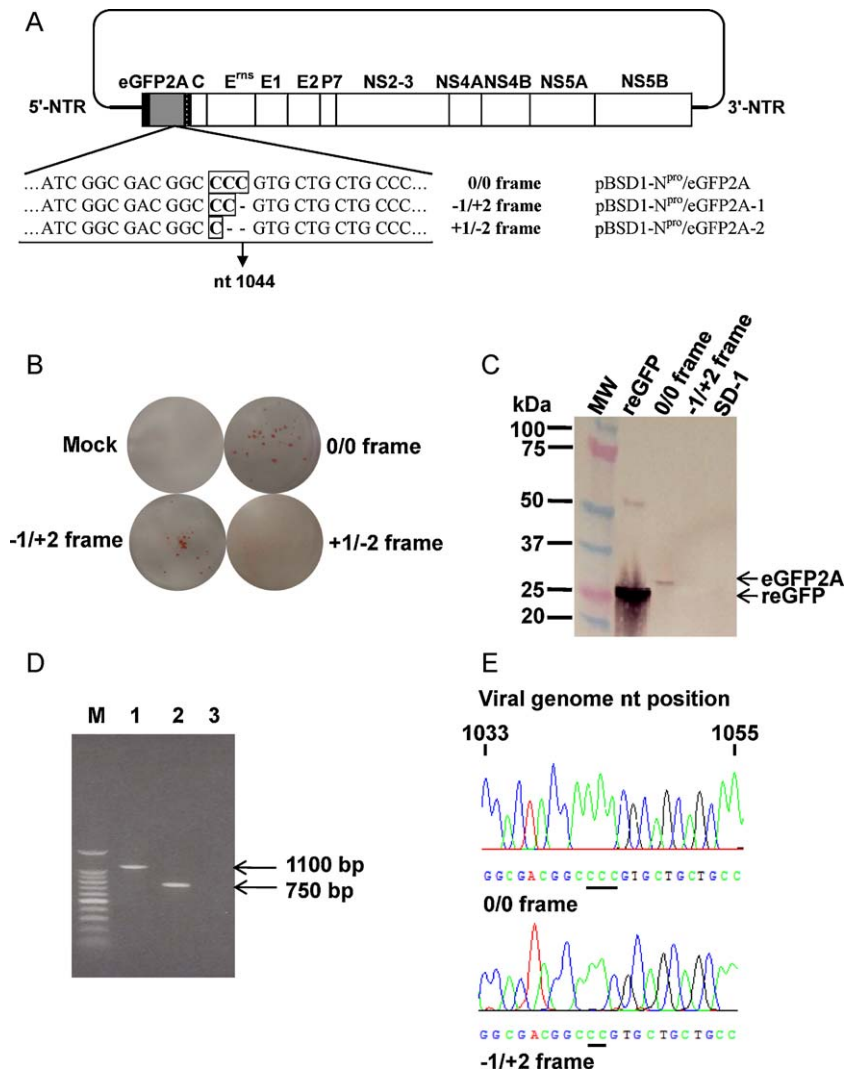


Fig. 5. Verification of the initiation of an additional $-1/+2$ ORF in $N^{\text{pro}}(1-19)/e\text{GFP}$ region. (A) Schematic representative of constructs used for *in vitro* transcription. Nucleotide sequences deduced from pBSD1- $N^{\text{pro}}/e\text{GFP2A}$, pBSD1- $N^{\text{pro}}/e\text{GFP2A-1}$ and pBSD1- $N^{\text{pro}}/e\text{GFP2A-2}$ are shown to represent 0/0, $-1/+2$ and $+1/-2$ frames, respectively. The nucleotide deletion was shown in a box and nucleotide position 1044 was labeled in the bottom. (B) Detection of infectious virus by focus forming assay in MDBK cells. Mock-infected MDBK monolayers were treated with complete MDEM medium without the *in vitro* transcribed RNA. The $+1/-2$ frame representing plasmid does not direct the regeneration of infectious virus. (C) Detection of green fluorescent protein by western blotting with monoclonal anti-GFP antibody, JL-8. MDBK cells were infected with SD-1, BSD1- $N^{\text{pro}}/e\text{GFP2A}$ (0/0 frame), or BSD1- $N^{\text{pro}}/e\text{GFP2A-c1044}\Delta$ ($-1/+2$ frame). The virus-infected cells were collected at 60 h p.i. Lane 1: Molecular mass standard (MW) in kilodaltons (kDa, indicated on the left); Lane 2: recombinant eGFP protein control; Lane 3 to Lane 4: 40 μg of lysate of MDBK cells infected by viruses representing 0/0 or $-1/+2$ frame; and Lane 5: 40 μg of lysates of SD-1-infected MDBK cells as a negative control. (D) Detection of the artificially introduced cytosine nucleotide deletion at nt 1044 of viral genome. Complementary DNA fragments amplified from viral RNA by RT-PCR. Primer pair of BVD424P and BVD1172 was utilized for RT-PCR. M: 1 kb DNA ladder; Lane 1. cDNA fragment amplified from viral RNA of $-1/+2$ frame-representing virus with an expected size of 1100 bp. Lane 2. cDNA fragments amplified from viral RNA of BSD1 with an expected size of 750 bp; and Lane 3: blank reaction (no templates) as negative control. (E) Single cytosine nucleotide deletion at nt 1044 was detected at the 3'-end of the eGFP coding region of the $-1/+2$ frame-representing virus genome. The shown nucleotide sequences of partial viral genomes were amplified from viral RNAs of viruses representing 0/0 or $-1/+2$ frame, respectively. The numbers show the nucleotide positions referring to the genomic sequence of BSD1- $N^{\text{pro}}/e\text{GFP2A}$.

However, in this specific case, the involvement of FMDV 2A^{pro} sequence in directing the generation of viable viruses is immediately excluded. The reason is simply due to the occurrence of a premature stop codon 54 nt upstream of the FMDV 2A^{pro} coding region in mutant viral genome. Following the original viral 0/0 ORF of the mutant viral genome, the protein translation is already ceased even before the ribosome can reach the FMDV 2A coding region to perform the ribosome skipping event. Considering that viral capsid protein is essential for formation of infectious viruses and must be synthesized first and then released from the viral polyprotein catalyzed by the 17 AA FMDV 2A^{pro} it is reasonable to postulate that an alternative $-1/+2$ ORF exists in the viral genome and this event must occur before the coding sequence of FMDV 2A^{pro}, namely in the $N^{\text{pro}}(1-19)/e\text{GFP}$ coding region. By using our

BAC-based reverse genetics system we find out that this event operating occurs in the $N^{\text{pro}}(1-19)$ region of the native BVDV SD-1, suggesting that the $-1/+2$ ORF of the viral genome probably has nothing to do with the heterologous eGFP insertion or FMDV 2A^{pro} sequence but seems to be an intrinsic characteristic of the native virus. The rescued virus is much lower than its parent virus in viral RNA, viral protein, and virus titer, indicating that the $-1/+2$ ORF of BVDV has a much lower efficacy than the original viral 0/0 ORF in viral protein translation.

By combination of the evidence, it was conclusive that the observed $-1/+2$ ORF in the $N^{\text{pro}}(1-19)$ region of BVDV SD-1 directs the polyprotein generation of the mutant virus. This can be achieved through a $-1/+2$ translational ribosome frameshift event or an $-1/+2$ internal translation initiation site that exists in the

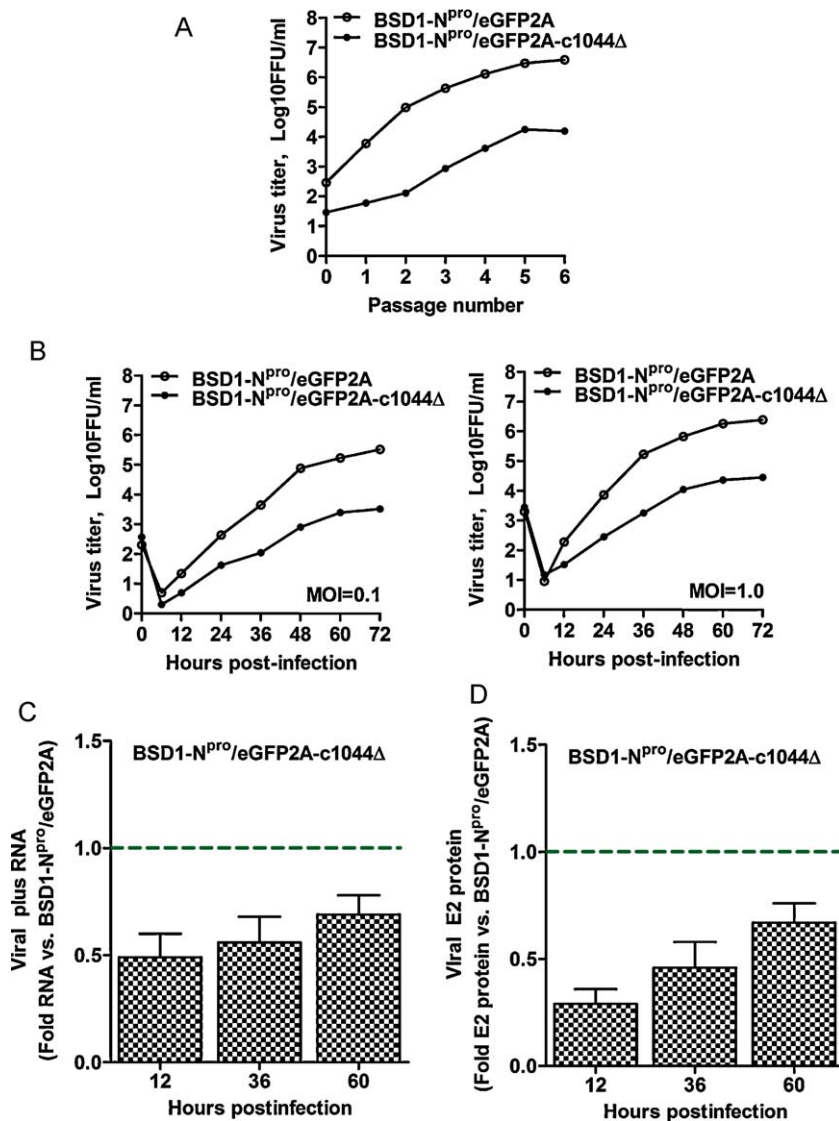


Fig. 6. Analysis of the mutation effect on growth property of BSD1-N^{pro}/eGFP2A-c1044Δ. (A) By defining the rescued virus as passage 0, BSD1-N^{pro}/eGFP2A-c1044Δ was passaged six more times in MDBK cells. The virus titer was determined for each passage and virus titer curve was generated by plotted against virus passage. The graph shows average values derived from three independently generated experiments. (B) MDBK cells were infected with either BSD1-N^{pro}/eGFP2A or BSD1-N^{pro}/eGFP2A-c1044Δ at an MOI of either 1.0 FFU/cell or 0.1 FFU/cell. At various time points p.i. as indicated, virus titers were determined. Viral growth curves were generated by plotted against time. Here, BSD1-N^{pro}/eGFP2A-c1044Δ and BSD1-N^{pro}/eGFP2A were designated by empty and solid circles, respectively. The graph shows average values derived from three independently generated experiments. (C) Viral genomic RNA was quantitatively measured. MDBK cells were infected with BSD1-N^{pro}/eGFP2A-c1044Δ or BSD1-N^{pro}/eGFP2A. Cells were harvested at indicated time points p.i., total cellular RNA was isolated and quantified for viral genomic RNA in quantitative RT-PCR. Here, total cellular RNA extracted from BVDV-negative MDBK cells were set as the negative control and the error bars represent the standard deviation of three independent experiments. (D) Viral E2 protein accumulation of BSD1-N^{pro}/eGFP2A-c1044Δ as compared to that of BSD1-N^{pro}/eGFP2A. Virus- and mock-infected MDBK cells were treated as described in Section 2. Viral protein accumulation was reflected by mean fluorescence intensity (MFI) of the E2-positive cells and is indicated in the plot. The error bars represent the standard deviation of three independent experiments.

N^{pro}(1–19) region of BVDV SD-1. Since the polyprotein translation of pestiviruses as well as other flaviviruses are initiated at the internal ribosome element site (IRES) the existence of a second internal translation initiation site at the 5'-end of N^{pro} region is much low. However, with current available evidence, this possibility cannot be excluded. Our next research focus will be directed to search for the exact translational ribosome frameshift site or the internal translational initiation site in the N^{pro}(1–19) region of BVDV SD-1 and to determine if the sequence and structure of BVDV 5'-NTR have any effects on this event.

Translational ribosome frameshift for gene expression has been reported existing in the life cycle of many RNA viruses such as retrovirus (Jacks and Varmus, 1985), coronaviruses (Brierley, 1995) and astroviruses (Marczinke et al., 1994). In 1994, the *flaviviridae*

family member, hepatitis C virus (HCV), was reported to encode an additional HCV polypeptide of around 16 kDa (Lo et al., 1994). Several following studies confirmed this observation and further showed that an additional HCV ORF overlaps the core gene in the +1 frame (core +1 ORF) (Choi et al., 2003; Roussel et al., 2003; Varakioti et al., 2002; Walewski et al., 2001; Xu et al., 2001). This polypeptide can be synthesized *in vitro* from the initiator codon of the viral polyprotein sequence followed by a +1 translational ribosome frameshift operating occurring in the coding region of core codons 8–14 (Vassilaki et al., 2008). Circulating anti-core +1 antibodies have been detected in HCV-infected individuals, suggesting that this protein is produced during natural HCV infection (Choi et al., 2003; Roussel et al., 2003; Varakioti et al., 2002; Walewski et al., 2001; Xu et al., 2001). These data together show that, besides

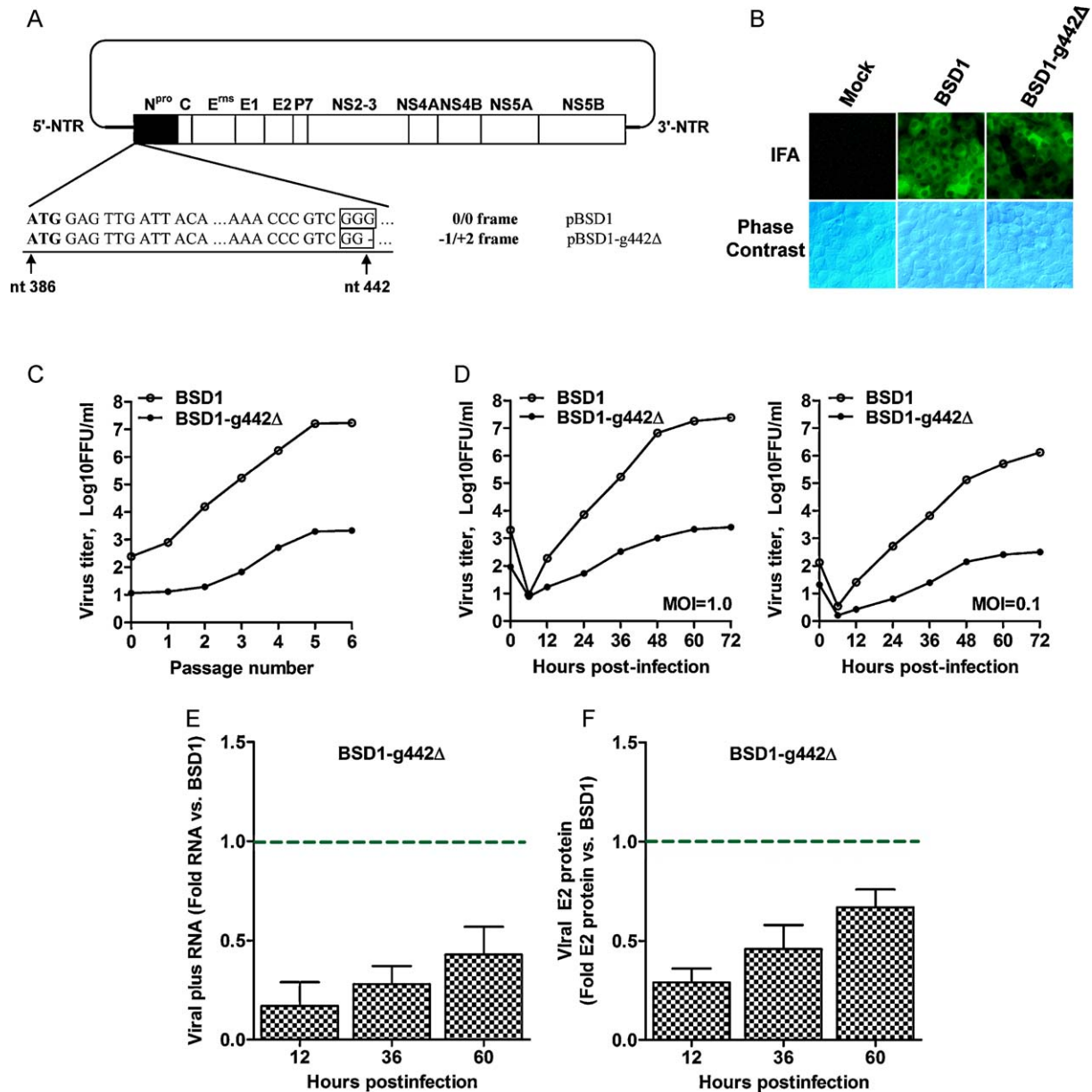


Fig. 7. An additional $-1/+2$ ORF initiates in viral N^{pro}(1–19) region of native BVDV SD-1. (A) Schematic representative of constructs pBSD1 and pBSD1-g442Δ that represent 0/0 and $-1/+2$ frames, respectively, for *in vitro* transcription. The initial codon of viral N^{pro} protein (nt 386–388) and the single guanine-nucleotide deletion (nt 442) was shown. (B) IFA of mock-, BSD1-, and BSD1-g442Δ-infected MDBK cells. The images were captured at 60 h p.i. The same views of IFA stained with Alexa 580 (upper panel) and of phase contrast (bottom panel) are shown. (C) After the rescue of BSD1-g442Δ (passage 0), the viruses were passaged additional six times in MDBK cells. The virus titer was determined for each passage and virus titer curve was generated by plotted against virus passage number. The graph shows average values derived from three independently generated experiments. (D) MDBK cells were infected with either BSD1 or BSD1-g442Δ at an MOI of either 1.0 FFU/cell or 0.1 FFU/cell. At various time points p.i. as indicated, virus titers were determined. Viral growth curves were generated by plotted against time. Here, BSD1 and BSD1-g442Δ were designated by empty and solid circles, respectively. The graph shows average values derived from three independently generated experiments. (E) Viral RNA genome was quantitatively measured in a time-course manner. MDBK cells were infected with BSD1 or BSD1-g442Δ. Cells were harvested at indicated time points p.i., total cellular RNA was isolated and quantified as described above in quantitative RT-PCR. The error bars represent the standard deviation of three independent experiments. (F) Accumulation of intracellular viral E2 protein of BSD1-g442Δ as compared to that of BSD1. Virus- and mock-infected MDBK cells were treated as described above. Accumulation of viral E2 protein was reflected by mean fluorescence intensity (MFI) of the E2-positive cells and is indicated in the plot. The error bars represent the standard deviation of three independent experiments.

its role in viral assembly, the core protein of HCV might play a pivotal role in viral pathogenesis (Brierley, 1995; Futterer et al., 1993; Jayakar and Whitt, 2002; Kobayashi et al., 2000; Latorre et al., 1998; Pavlakis and Felber, 1990; Stacey et al., 2000). In most recent years, researchers observed that translational ribosome frameshift event also exists in many other *flaviviridae* family viruses such as Dengue virus (Firth and Atkins, 2009; Firth et al., 2010), Japanese Encephalitis Virus (Melian et al., 2010) and West Nile virus (Youn et al., 2010). Although we cannot determine with current available

evidence that BVDV exhibits a translational frameshift event during its replication, it is possible that translational ribosome frameshift for gene expression is probably a common strategy that is applied by many virus members of all three genera in *flaviviridae* family to synthesize more viral proteins with their limited genetic materials. Specifically for BVDV SD-1, however, we noticed that an additional $-1/+2$ ORF in N^{pro}(1–19) region causes the generation of a peptide with a maximum size of 29 amino acids (data not shown). If there exists a translational ribosome frameshift site or an internal

translational initiation site in the N^{pro}(1–19) region and the biological relevance of this additional –1/+2 ORF during BVDV life cycle needs to be carefully investigated in the future.

Acknowledgments

We gratefully thank Charles M. Rice and Benno Woelk (The Rockefeller University) for their helpful suggestions to measure the fluorescence signal. We appreciate Kenny V. Brock (Auburn University) for kindly providing the reagents necessary to finish this study. We are grateful to Dr. Christine C. Dykstra (Auburn University) for her helpful discussion. We would like to give our thanks to John C. Dennis (Auburn University) and Allison C. Bird (Auburn University) for their technical assistance in fluorescence microscopy and flow cytometry, respectively.

This work was supported by the College of Veterinary Medicine, Auburn University.

References

- Baginski, S.G., Pevear, D.C., Seipel, M., Sun, S.C., Benetatos, C.A., Chunduru, S.K., Rice, C.M., Collett, M.S., 2000. Mechanism of action of a pestivirus antiviral compound. *Proc. Natl. Acad. Sci. U.S.A.* 97 (14), 7981–7986.
- Baril, M., Brakier-Gingras, L., 2005. Translation of the F protein of hepatitis C virus is initiated at a non-AUG codon in a +1 reading frame relative to the polyprotein. *Nucleic Acids Res.* 33 (5), 1474–1486.
- Bauhofer, O., Summerfield, A., Sakoda, Y., Tratschin, J.-D., Hofmann, M.A., Ruggli, N., 2007. Classical Swine Fever Virus N^{pro} interacts with interferon regulatory factor 3 and induces its proteasomal degradation. *J. Virol.* 81 (7), 3087–3096.
- Boulant, S., Becchi, M., Penin, F., Lavergne, J.P., 2003. Unusual multiple recoding events leading to alternative forms of hepatitis C virus core protein from genotype 1b. *J. Biol. Chem.* 278 (46), 45785–45792.
- Brierley, I., 1995. Ribosomal frameshifting viral RNAs. *J. Gen. Virol.* 76, 1885–1892 (Pt 8).
- Chen, Z., Rijnbrand, R., Jangra, R.K., Devaraj, S.G., Qu, L., Ma, Y., Lemon, S.M., Li, K., 2007. Ubiquitination and proteasomal degradation of interferon regulatory factor-3 induced by N^{pro} from a cytopathic bovine viral diarrhoea virus. *Virology* 366 (2), 277–292.
- Choi, J., Xu, Z., Ou, J.H., 2003. Triple decoding of hepatitis C virus RNA by programmed translational frameshifting. *Mol. Cell. Biol.* 23 (5), 1489–1497.
- Cristina, J., Lopez, F., Moratorio, G., Lopez, L., Vasquez, S., Garcia-Aguirre, L., Chunga, A., 2005. Hepatitis C virus F protein sequence reveals a lack of functional constraints and a variable pattern of amino acid substitution. *J. Gen. Virol.* 86, 115–120 (Pt 1).
- Deng, R., Brock, K.V., 1992. Molecular cloning and nucleotide sequence of a pestivirus genome, noncytopathic bovine viral diarrhoea virus strain SD-1. *Virology* 191 (2), 867–869.
- Donnelly, M.L.L., Luke, G., Mehrotra, A., Li, X., Hughes, L.E., Gani, D., Ryan, M.D., 2001. Analysis of the aphthovirus 2A/2B polyprotein 'cleavage' mechanism indicates not a proteolytic reaction, but a novel translational effect: a putative ribosomal 'skip'. *J. Gen. Virol.* 82 (5), 1013–1025.
- Dopf, J., Horiagon, T.M., 1996. Deletion mapping of the *Aequorea victoria* green fluorescent protein. *Gene* 173 (1 Spec No), 9–44.
- Fan, Z.C., Bird, R.C., 2008a. Generation and characterization of an N^{pro}-disrupted marker bovine viral diarrhoea virus derived from a BAC cDNA. *J. Virol. Methods* 151 (2), 257–263.
- Fan, Z.C., Bird, R.C., 2008b. An improved reverse genetics system for generation of bovine viral diarrhoea virus as a BAC cDNA. *J. Virol. Methods* 149 (2), 309–315.
- Fan, Z.C., Dennis, J.C., Bird, R.C., 2008. Bovine viral diarrhoea virus is a suitable viral vector for stable expression of heterologous gene when inserted in between N(pro) and C genes. *Virus Res.* 138 (1–2), 97–104.
- Fan, Z.C., Wang, H.H., 2009. Regeneration and characterization of a recombinant bovine viral diarrhoea virus and determination of its efficacy to cross the bovine placenta. *Virus Genes* 38 (1), 129–135.
- Firth, A.E., Atkins, J.F., 2009. Evidence for a novel coding sequence overlapping the 5'-terminal approximately 90 codons of the gill-associated and yellow head okavirus envelope glycoprotein gene. *Virol. J.* 6, 222.
- Firth, A.E., Blitvich, B.J., Wills, N.M., Miller, C.L., Atkins, J.F., 2010. Evidence for ribosomal frameshifting and a novel overlapping gene in the genomes of insect-specific flaviviruses. *Virology* 399 (1), 153–166.
- Funston, G.M., Kallioinen, S.E., de Felipe, P., Ryan, M.D., Iggo, R.D., 2008. Expression of heterologous genes in oncolytic adenoviruses using picornaviral 2A sequences that trigger ribosome skipping. *J. Gen. Virol.* 89 (2), 389–396.
- Futterer, J., Kiss-Laszlo, Z., Hohn, T., 1993. Nonlinear ribosome migration on cauliflower mosaic virus 35S RNA. *Cell* 73 (4), 789–802.
- Gil, L.H., Ansari, I.H., Vassilev, V., Liang, D., Lai, V.C., Zhong, W., Hong, Z., Dubovi, E.J., Donis, R.O., 2006. The amino-terminal domain of bovine viral diarrhoea virus N^{pro} protein is necessary for alpha/beta interferon antagonism. *J. Virol.* 80 (2), 900–911.
- Hilton, L., Moganeradj, K., Zhang, G., Chen, Y.-H., Randall, R.E., McCauley, J.W., Goodbourn, S., 2006. The N^{pro} Product of Bovine Viral Diarrhoea Virus inhibits DNA binding by interferon regulatory factor 3 and targets it for proteasomal degradation. *J. Virol.* 80 (23), 11723–11732.
- Horscroft, N., Bellows, D., Ansari, I., Lai, V.C.H., Dempsey, S., Liang, D., Donis, R., Zhong, W., Hong, Z., 2005. Establishment of a subgenomic replicon for Bovine Viral Diarrhoea Virus in Huh-7 Cells and modulation of interferon-regulated factor 3-mediated antiviral response. *J. Virol.* 79 (5), 2788–2796.
- Jacks, T., Varmus, H.E., 1985. Expression of the Rous sarcoma virus pol gene by ribosomal frameshifting. *Science* 230 (4731), 1237–1242.
- Jayakar, H.R., Whitt, M.A., 2002. Identification of two additional translation products from the matrix (M) gene that contribute to vesicular stomatitis virus cytopathology. *J. Virol.* 76 (16), 8011–8018.
- Kobayashi, T., Watanabe, M., Kamitani, W., Tomonaga, K., Ikuta, K., 2000. Translation initiation of a bicistronic mRNA of Borna disease virus: a 16-kDa phosphoprotein is initiated at an internal start codon. *Virology* 277 (2), 296–305.
- La Rocca, S.A., Herbert, R.J., Crooke, H., Drew, T.W., Wileman, T.E., Powell, P.P., 2005. Loss of interferon regulatory factor 3 in cells infected with classical swine fever virus involves the N-terminal protease, N^{pro}. *J. Virol.* 79 (11), 7239–7247.
- Latorre, P., Kolakofsky, D., Curran, J., 1998. Sendai virus Y proteins are initiated by a ribosomal shunt. *Mol. Cell. Biol.* 18 (9), 5021–5031.
- Lindenbach, B.D., Evans, M.J., Syder, A.J., Wolk, B., Tellinghuisen, T.L., Liu, C.C., Maruyama, T., Hynes, R.O., Burton, D.R., McKeating, J.A., Rice, C.M., 2005. Complete replication of hepatitis C virus in cell culture. *Science* 309 (5734), 623–626.
- Lindenbach, B.D., Rice, C.M., 2003. Molecular biology of flaviviruses. *Adv. Virus Res.* 59, 23–61.
- Lo, S.Y., Selby, M., Tong, M., Ou, J.H., 1994. Comparative studies of the core gene products of two different hepatitis C virus isolates: two alternative forms determined by a single amino acid substitution. *Virology* 199 (1), 124–131.
- Marczinke, B., Bloys, A.J., Brown, T.D., Willcocks, M.M., Carter, M.J., Brierley, I., 1994. The human astrovirus RNA-dependent RNA polymerase coding region is expressed by ribosomal frameshifting. *J. Virol.* 68 (9), 5588–5595.
- McMullan, L.K., Grakoui, A., Evans, M.J., Mihalik, K., Puig, M., Branch, A.D., Feinstone, S.M., Rice, C.M., 2007. Evidence for a functional RNA element in the hepatitis C virus core gene. *Proc. Natl. Acad. Sci. U.S.A.* 104 (8), 2879–2884.
- Melian, E.B., Hinzman, E., Nagasaki, T., Firth, A.E., Wills, N.M., Nouwens, A.S., Blitvich, B.J., Leung, J., Funk, A., Atkins, J.F., Hall, R., Khromykh, A.A., 2010. NS1' of flaviviruses in the Japanese Encephalitis Virus serogroup is a product of ribosomal frameshifting and plays a role in viral neuroinvasiveness. *J. Virol.* 84 (3), 1641–1647.
- Meyers, G., Ege, A., Fetzer, C., von Freyberg, M., Elbers, K., Carr, V., Prentice, H., Charleston, B., Schurmann, E.-M., 2007. Bovine Viral Diarrhoea Virus: prevention of persistent fetal infection by a combination of two mutations affecting Erns RNase and N^{pro} protease. *J. Virol.* 81 (7), 3327–3338.
- Pavlikis, G.N., Felber, B.K., 1990. Regulation of expression of human immunodeficiency virus. *New Biol.* 2 (1), 20–31.
- Rijnbrand, R., Bredenbeek, P.J., Haasnoot, P.C., Kieft, J.S., Spaan, W.J., Lemon, S.M., 2001. The influence of downstream protein-coding sequence on internal ribosome entry on hepatitis C virus and other flavivirus RNAs. *RNA* 7 (4), 585–597.
- Roussel, J., Pillez, A., Montpellier, C., Duverlie, G., Cahour, A., Dubuisson, J., Wychowski, C., 2003. Characterization of the expression of the hepatitis C virus F protein. *J. Gen. Virol.* 84 (Pt 7), 1751–1759.
- Ruggli, N., Bird, B.H., Liu, L., Bauhofer, O., Tratschin, J.D., Hofmann, M.A., 2005. N(pro) of classical swine fever virus is an antagonist of double-stranded RNA-mediated apoptosis and IFN-alpha/beta induction. *Virology* 340 (2), 265–276.
- Rumenapf, T., Stark, R., Heimann, M., Thiel, H.-J., 1998. N-Terminal protease of pestiviruses: identification of putative catalytic residues by site-directed mutagenesis. *J. Virol.* 72 (3), 2544–2547.
- Ryan, M.D., Drew, J., 1994. Foot-and-mouth disease virus 2A oligopeptide mediated cleavage of an artificial polyprotein. *EMBO J.* 13 (4), 928–933.
- Ryan, M.D., King, A.M., Thomas, G.P., 1991. Cleavage of foot-and-mouth disease virus polyprotein is mediated by residues located within a 19 amino acid sequence. *J. Gen. Virol.* 72 (Pt 11), 2727–2732.
- Sambrook, J., Russell, D., 2001. *Molecular Cloning: A Laboratory Manual*, 3rd ed.
- Seago, J., Hilton, L., Reid, E., Doceul, V., Jayatheesan, J., Moganeradj, K., McCauley, J., Charleston, B., Goodbourn, S., 2007. The N^{pro} product of classical swine fever virus and bovine viral diarrhoea virus uses a conserved mechanism to target interferon regulatory factor-3. *J. Gen. Virol.* 88 (Pt 11), 3002–3006.
- Stacey, S.N., Jordan, D., Williamson, A.J., Brown, M., Coote, J.H., Arrand, J.R., 2000. Leaky scanning is the predominant mechanism for translation of human papillomavirus type 16 E7 oncoprotein from E6/E7 bicistronic mRNA. *J. Virol.* 74 (16), 7284–7297.
- Stark, R., Meyers, G., Rumenapf, T., Thiel, H.J., 1993. Processing of pestivirus polyprotein: cleavage site between autoprotease and nucleocapsid protein of classical swine fever virus. *J. Virol.* 67 (12), 7088–7095.
- Tratschin, J.-D., Moser, C., Ruggli, N., Hofmann, M.A., 1998. Classical Swine Fever Virus leader proteinase N^{pro} is not required for viral replication in cell culture. *J. Virol.* 72 (9), 7681–7684.
- Varaklioti, A., Vassilaki, N., Georgopoulou, U., Mavromara, P., 2002. Alternate translation occurs within the core coding region of the hepatitis C viral genome. *J. Biol. Chem.* 277 (20), 17713–17721.
- Vassilaki, N., Boleti, H., Mavromara, P., 2008. Expression studies of the HCV-1a core+1 open reading frame in mammalian cells. *Virus Res.* 133 (2), 123–135.

- Vassilaki, N., Mavromara, P., 2003. Two alternative translation mechanisms are responsible for the expression of the HCV ARFP/F/core + 1 coding open reading frame. *J. Biol. Chem.* 278 (42), 40503–40513.
- Walewski, J.L., Keller, T.R., Stump, D.D., Branch, A.D., 2001. Evidence for a new hepatitis C virus antigen encoded in an overlapping reading frame. *RNA* 7 (5), 710–721.
- Xu, Z., Choi, J., Yen, T.S., Lu, W., Strohecker, A., Govindarajan, S., Chien, D., Selby, M.J., Ou, J., 2001. Synthesis of a novel hepatitis C virus protein by ribosomal frameshift. *EMBO J.* 20 (14), 3840–3848.
- Youn, S., Cho, H., Fremont, D.H., Diamond, M.S., 2010. A short N-terminal peptide motif on Flavivirus nonstructural protein NS1 modulates cellular targeting and immune recognition. *J. Virol.* 84 (18), 9516–9532.